Effect of Poly(acrylic acid) End-Group Functionality on Inhibition of Calcium Oxalate Crystal Growth

Andrew D. Wallace,[1] Ali Al-Hamzah,[1] Christopher P. East,[1,2] William O. S. Doherty,[2] Christopher M. Fellows[1]

[1]*School of Science and Technology, The University of New England, Armidale, New South Wales 2351, Australia*
[2]*Sugar Research and Innovation, Centre for Tropical Crops and Biocommodities, Queensland University of Technology, Brisbane, Queensland 4001, Australia*

Received 30 June 2009; accepted 23 October 2009
DOI 10.1002/app.31657
Published online 17 December 2009 in Wiley InterScience (www.interscience.wiley.com).

ABSTRACT: A number of series of poly(acrylic acids) (PAA) of differing end-groups and molecular weights prepared using atom transfer radical polymerization were used as inhibitors for the crystallization of calcium oxalate at 23 and 80°C. As measured by turbidimetry and conductivity and as expected from previous reports, all PAA series were most effective for inhibition of crystallization at molecular weights of 1500–4000. However, the extent of inhibition was in general strongly dependent on the hydrophobicity and molecular weight of the end-group. These results may be explicable in terms of adsorption/desorption of PAA to growth sites on crystallites. The overall effectiveness of the series didn't follow a simple trend with end-group hydrophobicity, suggesting self-assembly behavior or a balance between adsorption and desorption rates to crystallite surfaces may be critical in the mechanism of inhibition of calcium oxalate crystallization. © 2009 Wiley Periodicals, Inc. J Appl Polym Sci 116: 1165–1171, 2010

Key words: adsorption; atom transfer radical polymerization (ATRP); crystallization; polyelectrolytes

INTRODUCTION

A significant problem in the sugar industry is the formation of scale on the heating surfaces of tubes in evaporator units. In Australian sugar mills the most important intractable scales forming in the late stages of the evaporation process are calcium oxalate monohydrate (COM) and dihydrate (COD) and silica.[1] COM and COD together make up about 50 wt % and silica accounts for about 30 wt % of all scale formed in the fourth and fifth effects.[2] COM has a relatively high heat capacity (153 J K^{-1} mol^{-1})[3] which increases with increasing temperature,[4] making COM an effective insulator between the heat transfer surfaces and the sugar juice inside the tubes. The sources of COM and COD in sugar milling are primarily calcium hydroxide (added to the juice in the clarification stage), and oxalic acid, which is both present originally in the sugar cane and formed *in situ* by oxidation of sucrose.[5]

Poly(acrylic acid) (PAA) and poly(maleic acid) are used for scale control in the sugar industry.[6–9] The exact mechanism by which these polymers function is still poorly understood, but several mechanisms may plausibly play a role: chelation of calcium ions by PAA, specific adsorption of PAA to active sites on the surface of crystallites to retard growth or alter crystal habit, electrosteric stabilization of calcium oxalate crystallites by PAA, and nucleation of calcium oxalate crystallites by Ca^{2+}: PAA complexes.[6,10] Current research in the area of polymeric and low-molecular weight modifiers of crystal growth and habit points towards selective adsorption of the additive at the crystal/solution interface as the dominant mechanism of crystal action.[11] Most scale-forming minerals are crystal hydrates, the surface of which will comprise a continuous layer of structural water, and the thermodynamics and kinetics of the replacement of this structural water by electron-donating additive will be critical in determining selectivity and effectiveness.[12] In our previous work on PAA scale inhibitors prepared with various chain transfer agents, the nature of the end-groups were shown to affect both rate of calcium oxalate crystallization and the morphology of the final crystals, with hydrophilic end groups being most effective in inhibiting scale formation and long hydrophobic end groups being least effective.[10] In this work we investigate these effects further using PAA prepared by atom transfer radical polymerization (ATRP) of *tert*-butyl acrylate (BA) to give better control of molecular weight and end-group functionality.

Additional Supporting Information may be found in the online version of this article

Correspondence to: C. M. Fellows (cfellows@une.edu.au).

EXPERIMENTAL

The method for the ATRP polymerization of poly (*tert*-butyl acrylate) (PBA) in this study was slightly modified from the method described by Ma and Wooley.[13] Selective hydrolysis of *tert*-butyl groups was done via transesterification using trifluoroacetic acid (TFA) to give PAA.[14]. Initiators were chosen for their varying hydrophobicity and expected interactions in the model calcium oxalate system.

Initiators

Ethyl 2-bromoisobutyrate

Ethyl 2-bromoisobutyrate (EB, Aldrich 98%) was used as received. This species is widely used as an ATRP initiator for acrylates.[13,15]

Decyl 2-bromoisobutyrate (DB)

n-dodecanol (2.3 g) was added to 60 mL of dichloromethane in a 100 mL three-necked round bottomed flask. 2.2 g of triethylamine was added and the reaction was stirred for 30 min. The reaction was cooled on an ice bath and setup with an addition funnel, under nitrogen atmosphere. 2-bromoisobutyryl bromide (4.0 g) was dissolved in 20 mL dichloromethane (DCM) and added dropwise to the mixture over the next hour. The reaction was stirred in the ice bath for a further hour, and then allowed to warm to room temperature with stirring overnight. The product was washed sequentially with 100 mL 0.1 *M* NaOH, 100 mL 0.1 *M* HCl, 100 mL water, 100 mL saturated NaCl and dried with $MgSO_4$. ^{1}H-NMR of crude product indicated it contained ~25% of alcohol starting material. The crude product was purified via distillation under high vacuum to give the final product as a clear liquid (69% yield).

Hexyl 2-bromoisobutyrate (HB), Cyclohexyl 2-bromoisobutyrate (CB), and Hexadecyl-2-bromoisobutyrate

3.0 g hexanol, 2.9 g cyclohexanol, or 7.0 g cetyl alcohol was added to 120 mL of dichloromethane (DCM) in a 250 mL three-necked round bottomed flask. 4.4 g of triethylamine was added to the reaction and the mixture was stirred for half an hour. The reaction was cooled in an ice bath an place under a nitrogen atmosphere. 8.0 g of 2-bromoisobutyryl bromide was dissolved in 40 mL of DCM and added dropwise via an addition funnel over the period of an hour. The reaction was stirred in an ice bath for another hour and the allowed to warm to room temperature overnight. The product was washed consecutively with 200 mL aliquots of 0.1 *M* NaOH, 0.1 *M* HCl, distilled water and saturated NaCl. The product was dried over $MgSO_4$. ^{1}H-NMR of the crude product indicated small amounts of starting material and DCM. The product was distilled under high vacuum using a Kugelohr to give 80% yield (HB), 79% yield (CB), and 68% yield (HDB), respectively.

Polymer

tert-butyl acrylate

tert-Butyl acrylate (BA, Aldrich 98%) was washed twice with 0.05 *M* NaOH, followed by two washes with water. After drying over $CaCl_2$, BA was distilled under reduced pressure, only the middle fraction was collected. The purified monomer was stored over calcium hydride at 0°C until required.

CuBr

CuBr (98% Aldrich) was stirred in glacial acetic acid for 24 hrs under a N_2 atmosphere, washed with ethanol and diethyl ether, and then dried in a vacuum desiccator at 70°C for 3 days. The purified CuBr, which was white in color, was stored in a sealed container until required.

N,N,N′,N″,N″-pentamethyldiethylenetriamine

N,N,N′,N″,N″-pentamethyldiethylenetriamine (PMDETA, Aldrich 99%) was used as received.

Polymerization of BA

CuBr, BA and ligand were added to a 10 mL reaction flask and frozen. Initiator was added to the frozen mass and the mixture subjected to three freeze/pump/thaw cycles before sealing under vacuum. The mixture was thawed and mixed in a vortex mixer. The flask was heated in a temperature-controlled oil bath at 60°C or 90°C until a solid mass of relatively uniform color was obtained. The flask was opened and the resulting polymer was dissolved up in ~ 5 mL of tetrahydrofuran (THF) and filtered through a short column containing celite/Al_2O_3 packing. The THF was removed in a rotary evaporator and the polymer mass was redissolved in 5 mL of methanol and poured into a Petri dish. The PBA was precipitated via slow addition of water until cloudiness was apparent and allowed to stand covered for ~ 4 hr. The supernatant was decanted and the precipitated PBA dried under air at 35°C for several days. Typical conditions for the polymerizations are given in Table I, together with the theoretical number average molecular weight (M_n) expected in each synthesis with ideal controlled radical polymerization. In most cases, the molecular weights measured for the polymers were similar to the theoretically predicted M_n.

TABLE I
Reaction Conditions for Polymerization of *tert*-Butyl Acrylate by ATRP, $T = 90°C$

	Molar ratio: Initiator				
Experiment	Monomer	Ligand (PMDETA)	Catalyst (CuBr)	t (hr)	M_n
EB 1	21	0.87	1.18	>12	2,910
EB 2	51	0.98	1.09	>12	6,090
EB 3	72	0.91	1.18	>12	9,400
HB 1	24	0.97	1.03	>24	3,270
HB 2	51	0.99	1.00	>24	6,810
HB 3	79	0.99	1.00	>24	10,320
CB 1	24	0.93	1.15	15	3,300
CB 2	46	0.84	1.18	15	6,090
CB 3	84	0.99	1.12	15	10,980
DB 1	27	0.98	1.03	7	3,710
DB 2	49	0.97	1.02	6	6,640
DB 3	78	1.00	1.00	26	10,340
HDB 1	16	1.60	1.60	18	2,628
HDB 2	31	1.00	1.00	25	4,301
HDB 3	50	1.00	1.00	25	6,747
HDB 4	97	0.94	0.94	38	13,954
HDB 5	217	1.00	1.00	39	28,239

The PBA obtained was characterized by ^{1}H-NMR spectroscopy. While the majority of the end-group proton environments in the PBA prepared overlap the main chain of the polymer, the protons adjacent to the sp^3 oxygen in the terminal ester (4.1 ppm) and the methyl groups derived from the butyrate group of the initiator (1.1 ppm) occupy distinct positions and may be used to estimate the molecular weight of the PBA. Published Mark-Houwink-Sakurada parameters are not applicable to these polymers due to their low-molecular weight and the large relative size of their end-groups, so the conventional procedure of measuring molecular weight by gel permeation chromatography (GPC) could not be applied.

Selective Hydrolysis of PBA to PAA

1.5 g PBA (11.5 mmol) was dissolved in 30 mL dichloromethane (DCM) and stirred with excess trifluoroacetic acid (TFA) (6.7 g, 57.5 mmol) for 12 hr at room temperature. The PAA formed as an insoluble mass collecting on the flask sides and stirrer bar. At completion the excess DCM and TFA were decanted and the resulting polymer dried under vacuum. Selected samples of PAA were characterized with ^{1}H-NMR in in d_6-dimethyl sulfoxide (Aldrich 99.9% D) to verify the removal of the *t*-butyl ester peak at 1.4 ppm and that the end-group ester was not removed.

Unselective hydrolysis of PAA end-groups

Hydrolysis of the PAA end-groups was done to prepare a PAA series with a hydrophilic carboxylic acid end-group. 0.5 g of PAA, 2 mL of 10 *M* HCl and 20 mL of water refluxed for 3–4 hr, allowed to cool and poured into a Petri dish. The mixture was evaporated to dryness over several days at 35°C. The resulting polymer was purified by redissolving in a small amount of water, washing with DCM, and drying under vacuum. Total hydrolysis of end-groups was confirmed for representative samples with ^{1}H-NMR in d_6-dimethyl sulfoxide.

Polymer characterization

Gel permeation chromatography (PBA)

Reagent grade tetrahydrofuran (THF, Aldrich 99%) inhibited with 0.025% butylated hydroxytoluene was distilled over sodium to remove inhibitor and any water. The solvent was filtered and degassed with a Millipore 0.45 μm solvent filter and used within 48 hr of preparation. 2.5 mg of each polymer sample (PBA and polystyrene standards) was dissolved in 1 mL THF and allowed to stand for a minimum of 12 hr before injection. Samples were filtered through a 0.45 μm syringe filter before injection. GPC was performed with a Waters 1525 HPLC Binary pump fitted with a Reodyne 50 μL manual injector and Waters 2414 RI detector using a Waters HR2 Styragel (7.8 × 300 mm) column maintained at 30°C. THF eluent was used at a flow rate of 1 mL min^{-1}. Polymers were analyzed using PSS WinGPC processing software (version 6).

The GPC column was initially calibrated using a series of eight polystyrene standards (PSS) from M_n 376 to M_n 50,000 g mol^{-1}. M_n values from this universal calibration were higher than both the theoretical values and the ^{1}H-NMR estimates. This is not surprising as the entire calibration range over which the Mark-Houwink-Sakurada parameters were established ($7.4 \times 10^4 - 5.4 \times 10^6$) lies outside the predicted molecular weights of the products.[16]

Column calibration with ^{1}H-NMR estimates

NMR Spectra were recorded in solvent specified on a Bruker Avance 300 NMR spectrometer at 25°C (Fig. 1). A calibration curve was determined using five of the experimental PBA samples from Series 1 with narrow polydispersities (EB5-8, EB13). M_n values from ^{1}H-NMR estimates were used to plot the curve. M_n results from this method of calibration were only considered an estimate, but were adequate for determining the polydispersity of the samples. M_n values from this calibration were in reasonable agreement with the theoretical expected value for all polymers tested.

Average molecular masses and polydispersities were determined for all PBA before hydrolysis using a combination of GPC and ^{1}H-NMR methods.

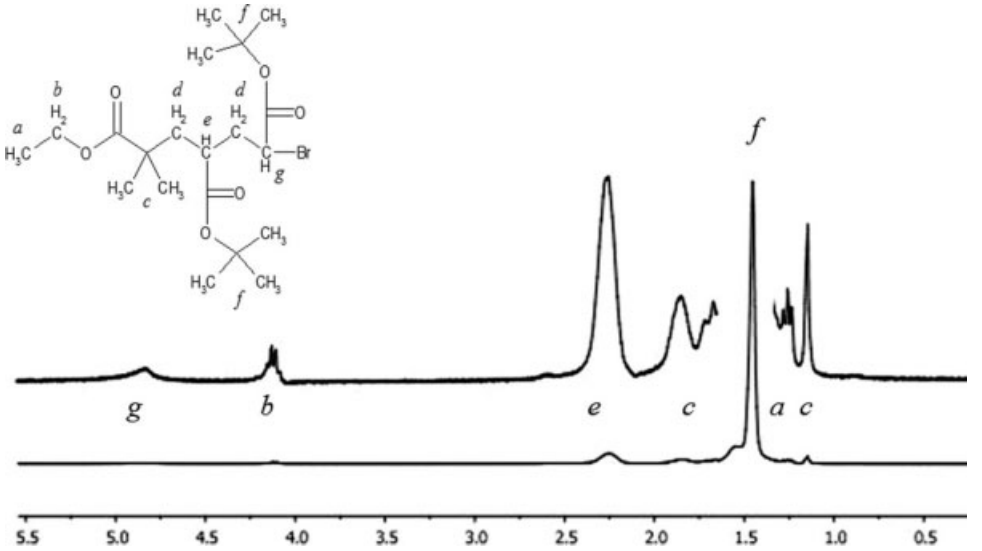

Figure 1 ^{1}H-NMR spectrum of PBA prepared by ATRP (Experiment EB9).

Average molecular masses and polydispersities of the final PAA series were determined from the PBA values.

PAA terminated with ethyl isobutyrate (EB), *n*-decyl isobutyrate (DB), *n*-hexyl isobutyrate (HB), cyclohexyl isobutyrate (CB) *n*-hexadecyl isobutyrate (HDB), and isobutyric acid (N) were prepared. The estimated molecular mass averages and polydispersities for all PAA prepared are given in the Supporting Information (Table S1).

Conductivity

Continuous measurement of ion depletion in solution resulting from crystallization may be achieved by monitoring conductivity. Calcium ion-selective probes are commercially available and have been used in several other studies[17] but due to concern about scale adhesion to the probe membrane and reproducibility were not used in this work. In multiple salt systems with multivalent ions, ion contributions to conductivity are not additive. For example, in model COM systems where $Na_2[Ox]$ and $CaCl_2$ are used various ionic associations occur and actual conductivity measurements may be significantly higher or lower than predicted values based on additive model.[18] However, the focus of interest in this work was not absolute ion concentrations, but relative rates of ion consumption in relation to crystal growth. The relationship between conductivity and COM concentration under the conditions used was determined to be linear under conditions of constant NaCl concentration, indicating the conductivity measurement could be used directly to measure relative ion consumption rates. A $4.0 \times 10^{-4}M$ NaCl solution was prepared quantitatively and the conductivity was measured. To this solution COM was added in 0.5–2.0 ppm increments with stirring and conductivity was measured after 5 min equilibration time. Conductivity was measured with a conductivity probe and meter (Beta 81, CHK Engineering). The meter was calibrated using KCl solutions by a standard procedure.[3]

A typical conductivity curve is given in Figure 2, showing the induction time (the cross-over point between the line of initial conductivity and the tangent to the curve over the period of significant decline) and the crystallization time (the cross-over point between this same tangent and the final steady-state conductivity value).

Turbidity

Measuring the increase in turbidity against time is a standard method of testing scale inhibitors.[10] UV-vis spectrophotometry can be used to measure turbidity

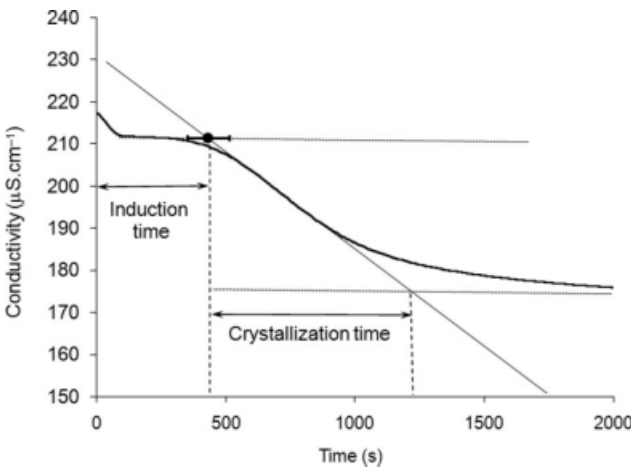

Figure 2 Typical conductivity curve (23°C, CB 3).

in solutions where absorbance is negligible.[19] The test solution was pumped continuously through a Pye Unicam 10 mm Quartz flow cell using a Gilson peristaltic pump with 4 mm silicon tubing, and then returned to the main mixture. The flow cell was mounted in a thermostatted Pye Unicam spectrophotometer SP6-550 and absorbance was recorded at 900 nm. Temperature was recorded using a resistance thermometer sealed into 4 mm internal diameter thin wall glass tubing. Analogue outputs from all sensors were digitally converted using a Picolog A/D Converter 16 (16 bit) and Picolog recording software and data was acquired every 10 s.

Experimental method

Two solutions, 0.137 *M* $Na_2C_2O_4$ and 0.137 *M* $CaCl_2$, were prepared. These solutions and the R/O water used were filtered and degassed using a 0.45 μm Millipore solvent filter. PAA solutions were prepared as 0.015 g in 20 mL water, 3+ days before use. 246.0 g of R/O water was added to a new 400 mL beaker free from scratches and imperfections and stirred at a constant rate. 1.00 mL of $CaCl_2$ solution was added and after 2 min equilibration the UV-vis spectrophotometer was zeroed. 2.00 mL of PAA solution to give a final concentration of 6 ppm, followed by 1.00 mL of Na_2 C_2O_4 solution was then added. After each experiment all equipment was flushed multiple times with weak acid followed by R/O water. All tests were carried out at 23°C or 80°C.

RESULTS AND DISCUSSION

Results obtained for induction times measured at 23°C are given in Figure 3. The induction times for each individual polymer are given in the Supporting Information (Table S2).

No lines have been drawn in Figure 3 either as empirical fits or "guides for the eye" to avoid imposing a greater degree of order than is warranted by the data. For all series, induction time was strongly dependent on molecular mass, with $M_n = 1500$–4000 showing the longest induction times. Although the relevant data set is small, no significant differences were observed in the inhibition behavior of high PDI and low PDI DB-terminated PAA, suggesting the role of polydispersity may be relatively minor.

The time taken from the onset of crystallization until the achievement of a final "steady state" absorbance or conductance value was also measured, giving an estimate of the impact of the PAA on crystal growth.

The induction time data obtained were examined in two different ways to search for statistically significant trends.

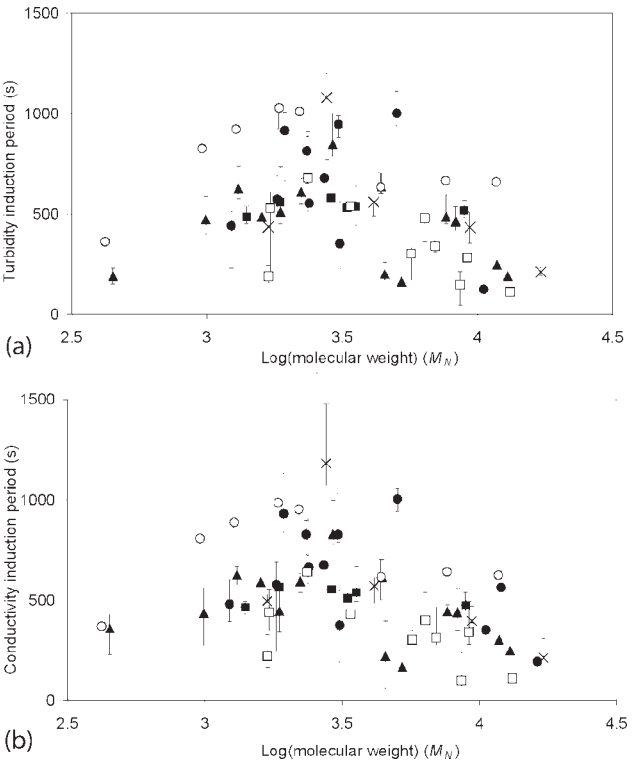

Figure 3 Inhibition periods determined by (a) turbidity and (b) conductivity for PAA terminated with EB (▲), HB (■), CB (□), DB (●), HDB (×), and fully hydrolyzed (N, ○) end-groups.

Firstly, polynomials were fitted to the curve of all induction time data as a function of molecular weight (with end-group subtracted), separately for both the absorbance and the conductance data sets. For each data point, the difference was then found between this predicted induction time and the actual induction time.Confidence intervals were then determined for these differences using standard statistical methods in Microsoft Excel (Table S3). EB, HB, and CB-terminated PAA gave induction times shorter than average, with CB significantly poorer than HB, while DB and HDB-terminated PAA and fully hydrolyzed PAA gave longer than average induction times. The confidence intervals obtained were highly dependent on the number of data points, so only the reduced induction times for HB and CB and the long induction times for fully-hydrolysed PAA can be considered statistically significant. The value of this treatment may be gauged by the high degree of similarity between the conductivity and turbidity data sets.

The crystallization time values provide an indication of rate of growth of the crystals after the end of the induction period. There is a positive correlation between these values and the measured induction times (Fig. 4).

The overall trend in inhibition behavior over both the induction and crystallization periods is

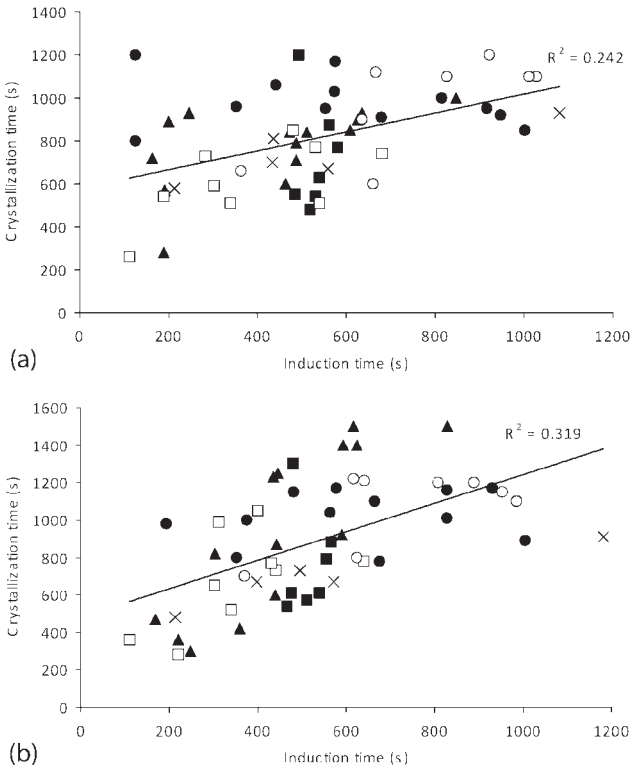

Figure 4 Correlation between induction times and crystallization times determined by (a) turbidity and (b) conductivity for PAA terminated with EB (▲), HB (■), CB (□), DB (●), HDB (×), and fully hydrolyzed (N, ○) end-groups.

consistent with a model where PAA operates by adsorption/desorption to active sites on the growing calcium oxalate crystallites. These active sites are defect structures on the surfaces, so it is not surprising that PAA shows effects at concentrations much less than required to completely cover the crystallite surfaces. A molecular mass dependence on effectiveness is expected, as small chains will desorb rapidly while large chains will not relax sufficiently to cover the active site within the required timeframe, and this optimum mass of the polymer has been found to lie between 2000 and 4000 g/mol for PAA.[20] The distribution and spacing of the ions on different surfaces of the crystallites will also influence the degree to which PAA will adsorb: in COD, the {010} faces present chiefly oxalate ions, while a dense pattern of calcium ions is presented at {100} faces, making PAA adsorption much more favorable to the latter.[21] Two separate influences of a hydrophobic end-group on adsorption/desorption may be postulated:

A hydrophobic end-group may encourage desorption, as it provides a "loose end," not bound to the crystal(lite) surface, from which desorption may begin. However, interactions between the hydrophobe and the aqueous phase are also unfavorable, so the presence of a hydrophobe will encourage the polymer to remain in an environment where polymer concentration is high enough that end-groups may self-associate to remove themselves from the aqueous phase. This trend would be expected to become more pronounced as the length of the end-group increases, possible explaining the minimum in induction time and crystallization time at intermediate end-group sizes. Self-association of the cyclohexyl isobutyrate end-groups would be expected to be less probable than self-association of the *n*-hexyl isobutyrate end-groups due to the more rigid structure and smaller surface area of the former, possibly explaining the poorer performance of CB-terminated in comparison to HB-terminated PAA.

The role of both hydrophilic and hydrophobic end-groups in modifying PAA would then be to encourage adhesion to growing crystallite surfaces, retarding growth and modifying crystal habit. As the self-assembly of hydrophobes in aqueous solution is entropically driven by the reduction of restrictions on the motion of water, the effectiveness of hydrophobes in maintaining PAA adhesion to crystallite surfaces would be expected to increase, and accordingly a subset of the PAA prepared were investigated at 80°C (Table II). No induction times could be observed in these experiments: the systems either remained at a constant conductivity over the entire course of the experiment, or underwent immediate rapid change. The trend in observed crystallization times was significantly different from the results obtained at 23°C.

At the PAA concentration of 6 ppm used at 23°C, all polymers gave very significant inhibition at 80°C, such that to discriminate between them it was necessary to reduce the concentration of PAA employed. When this was done, the most effective PAA were found to be the chains terminated by the relatively short hexyl isobutyrate hydrophobe. A possible explanation for the reduction in relative effectiveness may lay in the increasingly unfavorable solubilization of these PAA as temperature increases, which

TABLE II
Crystallization Times Measured at 80°C

	1.5 ppm PAA	400 ppb PAA
Sample	Conductance (s)	
EB 1	[a]	310 ± 10
HB 1	[a]	450 ± 180
CB 1	[a]	350 ± 140
DB 1	320 ± 120	[b]
HDB 3	290 ± 120	[b]
N 5	[a]	170 ± 50

[a] Indicates that no significant decrease in conductivity was observed over the 3000 s term of the experiment.
[b] Indicates that no experiment was performed under this set of conditions.

may retard transport of the PAA with longer hydrophobes from micelles into solution to interfaces to such an extent that their effective concentration on crystallite surfaces is no longer effective to inhibit growth. Observations of significant foaming in related experiments with HDB1 at 100°C suggest that the surface activity of PAA terminated with the longer alkyl isobutyrates is significant. No clear evidence of self-assembly was observed in preliminary experiments attempting to determine micellization parameters of the hydrophobe-terminated PAA.

The induction time data reported here can be correlated with effects on calcium oxalate hydrate speciation and morphology at 23°C observed by scanning electron microscopy.[22] Dramatic increases in the amount of COD were observed for polymers with moderately-sized hydrophobic end-groups (HB and CB) while shorter and longer hydrophobes gave predominantly COT. As COT is the phase formed initially according to Ostwald's rule, these results suggest adhesion of PAA to the growing crystal surface is weak at this temperature for HB and CB end-groups, allowing rearrangement or redissolution to form COD; but strong interactions between the surface and PAA with longer hydrophobic end-groups or fully hydrolyzed PAA maintain the initially precipitated calcium oxalate as COT.

CONCLUSION

The effectiveness of PAA scale inhibitors in inhibiting the onset of measurable calcium oxalate precipitation in a model system at room temperature was found to be greatest at molecular weights between 1700 and 3300, reproducing earlier findings. More significantly, a strong effect of the end-group was found independent of molecular weight, with PAA terminated with longer hydrophobes such as hexadecyl isobutyrate or with carboxylic acid end groups showing better performance than chains with intermediate-length hydrophobes both in terms of induction time and the rate of growth of crystals after the induction period. Cyclohexyl butyrate-terminated inhibitors performed more poorly than *n*-hexyl butyrate-terminated inhibitors, suggesting that association of the hydrophobes as they increase in size is suppressing desorption that would otherwise be encouraged by incorporation of the hydrophobic end-groups. These results were interpreted in terms of the degree to which the scale inhibitors could adsorb to the surface. At 80°C, the effectiveness of the inhibitors terminated with short hydrophobes improved, in line with the expected effect of increasing temperature on surfactant solubility, but the effectiveness of the inhibitors terminated with long hydrophobes declined, which was provisionally attributed to micellization phenomena retarding transport of polymer through the aqueous phase and preventing sufficient coverage of active sites on the crystal surfaces.

References

1. Yu, H.; Sheikholeslami, R.; Doherty, W. O. S. AIChE J 2005, 51, 1214.
2. Yu, H.; Sheikholeslami, R.; Doherty, W. O. S. Ind Eng Chem Res 2002, 41, 3379.
3. Lyde, D. R. CRC Handbook of Chemistry and Physics, 83rd ed.; CRC Press: Boca Raton, Florida, 2002–2003.
4. Latimer, W. M.; Schutz, P. W.; Hicks, J. F. G. J Am Chem Soc 1933, 55, 968.
5. Doherty, W. O. S. Ind Eng Chem Res 2006, 45, 642.
6. Senogles, E.; Doherty, W. O. S.; Crees, O. L. Encyclopedia of Polymer Science and Technology; Kroschwitz, J., Ed. Wiley: Boca Raton, 1996; pp 7587–7594.
7. Batson, D.B. Presented at 38th Conference, Cairns, Queensland Proceedings; Sturgess, O.W., Ed.; Watson Ferguson and Company: Brisbane, Queensland, Australia; Queensland Soc. of Sugar Cane Technol 1971, 207–210.
8. Doherty, W. O. S.; Crees, O. L.; Senogles, E. Cryst Res Technol 1995, 30, 791.
9. Clarke, S. J. Proc Aust Soc Sugar Cane Technol 1989, 11, 191.
10. Doherty, W. O. S.; Fellows, C. M.; Gorjian, S.; Senogles, E.; Cheung, W. H. J Appl Polym Sci 2004, 91, 2035.
11. Sikiric, M. D.; Füredi-Milhofer, H. Adv Colloid Interface Sci 2006, 128, 135.
12. Füredi-Milhofer, H.; Sikiric, M.; Tunik, L.; Filipovic-Vincekovic, N.; Garti, N. Int J Mod Phys B 2002, 16, 359.
13. Ma, Q.; Wooley, K. L. J Polym Sci Part A: Polym Chem 2000, 38, 4805.
14. Schnitter, M.; Engelking, J.; Heise, A.; Miller, R. D.; Menzel, H. Macromol Chem Phys 2000, 201, 1504.
15. Moad, G.; Solomon, D. H. The Chemistry of Radical Polymerization; Elsevier: New York, 2006.
16. Mrkvickova, L.; Danhelka, J. J Appl Polym Sci 1990, 41, 1929.
17. Shih, W.-Y.; Albrecht, K.; Glater, J.; Cohen, Y. Desalination 2004, 169, 213.
18. Haselhuhn, F.; Kind, M. Chem Eng Technol 2003, 26, 347.
19. Tantayakom, V.; Sreethawong, T.; Fogler, H. S.; De Moraes, F. F.; Chavadej, S. J. Colloid Interface Sci 2005, 284, 57.
20. Binglin, Y. Water Treatment 1989, 4, 257.
21. Tunik, L.; Addadi, L.; Garti, N.; Furedi-Milhofer, H. J Cryst Growth 1996, 167, 748.
22. East, C. P.; Alhamzah, A.; Wallace, A. G.; Doherty, W. O. S.; Fellows, C. M. J Appl Polym Sci 2010, 115, 2127.